Langmuir
Article
pubs.acs.org/Langmuir

Quinoacridine Derivatives with One-Dimensional Aggregation-Induced Red Emission Property

Iqbal Javed, Tianlei Zhou, Faheem Muhammad, Jianhua Guo, Hongyu Zhang,* and Yue Wang*

State Key Laboratory of Supramolecular Structure and Materials, College of Chemistry, Jilin University, Changchun 130012, P. R. China

Supporting Information

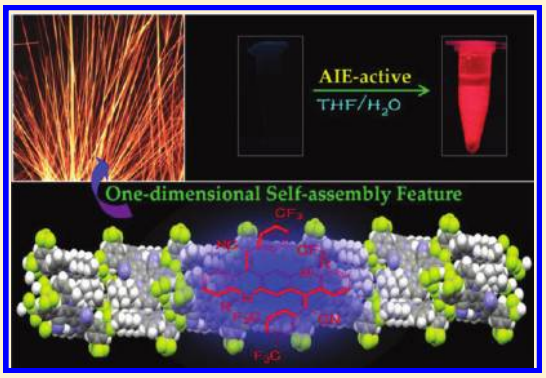

ABSTRACT: A new series of acceptor−donor−acceptor (A−D−A) type quinoacridine derivatives (**1**−**3**) with aggregation-induced red emission properties were designed and synthesized. In these compounds, the electron-withdrawing 2-(3,5-bis(trifluoromethyl)phenyl)acetonitrile groups act as electron-accepting units, while the alkyl-substituted conjugated core acts as electron-donating units. The restriction of intramolecular rotation was responsible for the AIE behavior of compounds **1**−**3**. All compounds were employed as building blocks to fabricate one-dimensional (1-D) organic luminescent nano- or microwires based on reprecipitation or slow evaporation approaches. Morphological transition from zero-dimensional (0-D) hollow nanospheres to 1-D nanotubes has been observed by recording SEM and TEM images of aggregated sates of compound **2** in THF/H$_2$O mixtures at different aging time. It was demonstrated that the synthesized compounds with different lengths of alkyl chains displayed different wire formation properties. The single-crystal X-ray analysis of compound **2** provided reasonable explanation for the formation of 1-D nano- or microstructures.

INTRODUCTION

Micro- and nanoscale materials such as nanowires, nanoparticles, and nanorods represent attractive building blocks for the fabrication of functional micro- and nanoscale devices.[1] The quantum size effect of micro- and nanostructured inorganic semiconductors could induce new optical and electronic properties compared with those of common bulk materials.[2] Especially, one-dimensional (1-D) nanostructures have attracted great attention due to the high aspect ratio which leads to fascinating physical and chemical properties.[3] The 1-D assembly of organic functional molecules on various substrates offers a useful strategy for the construction of well-defined functional nanoscale materials which are potential candidates of active components in gas sensor, organic light-emitting diodes (OLED), organic field effect transistor (OFET), optical waveguide fibers, photodetectors, and solar cells, etc.[4−9] Recently, it was demonstrated that some π-conjugated small organic molecules could be employed as building blocks to assemble supramolecular 1-D nanostructures.[10] However, the controlling and understanding of anisotropic aggregation of small organic molecules used for constructing 1-D micro- and nanomaterials with well-defined structures remains a challenge.[11] To obtain desirable organic nanomaterials for optical and electronic applications, focus should be on the design and synthesis of functional organic building blocks and development of 1-D self-assembly.

1-D luminescent nano/microwires formed by π-conjugated organic molecules are attracting a lot of attention due to that these highly ordered functional materials often possess intriguing optical and electronic properties. In particular, materials exhibiting red emission in their aggregated or solid state might be useful in the field of efficient OLEDs, biosensors, and biolables.[12,13] However, the assembly of highly efficient red emitting organic nano/microwires is still an issue as most of red emissive organic molecules were provided with aggregation-caused quenching (ACQ) characteristic in solid state. The ACQ effect has greatly limited the scope of the device applications of organic luminophors. In 2001, Tang and coworkers proposed the concept of aggregation-induced emission (AIE),[14−17] the phenomenon in which compounds are nonemissive in solution form but become emissive in the aggregated state. Since this pioneering work, a great deal of effort has been invested in developing organic compounds with AIE properties and understanding the mechanism of the AIE phenomenon. The studies on AIE opened a new route to develop highly efficient luminescent organic materials in solid state, especially for the high performance organic electroluminescent (EL) materials, which usually suffer from the severe ACQ effect. Therefore, the design and synthesis of organic conjugated molecules that simultaneously possess AIE property and 1-D assembly feature will lead to the generation of 1D organic nano/micro materials with high fluorescent

Received: July 18, 2011
Revised: December 4, 2011
Published: December 7, 2011

efficiency. Recently, we have successfully fabricated luminescent nano/microwires based on quinacridone derivatives (QA).[18] QA derivatives are highly emissive in dilute solutions, however, the produced nano/microwires exhibited very low fluorescent quantum yields (0.19−2.0%) due to the ACQ effect. To pursue strong luminescence organic nano/microwires, the exploration of QA-based molecules which retain 1-D assembly feature and have AIE property have been performed. In the present study, we designed a new series of red emitting AIE active compounds (**1**−**3**) with 1-D assembly properties by incorporating two electron-withdrawing 2-(3,5-bis(trifluoromethyl)phenyl)-acetonitrile units at the carbonyl position of alkyl-substituted QA (Scheme 1 and Figure 1). To deeply understand the relationship between the molecular structure and properties, we systematically studied the optical, AIE, 1-D assembly properties, and morphology transition characteristics of these compounds. The 1-D self-assembling behavior of the compounds **1**−**3** has been further supported by single-crystal structure analysis.

Scheme 1. Synthesis Procedure of 2-(3,5-Bis(trifluoromethyl)phenyl)acetonitrile Derivatives 1−3

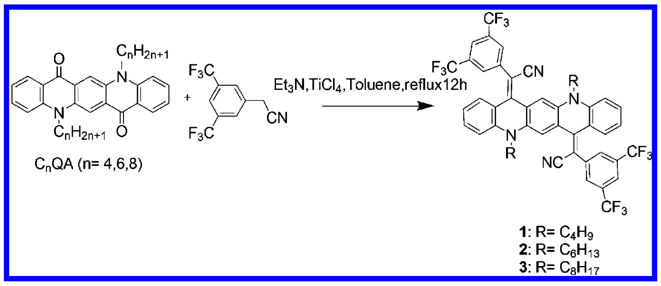

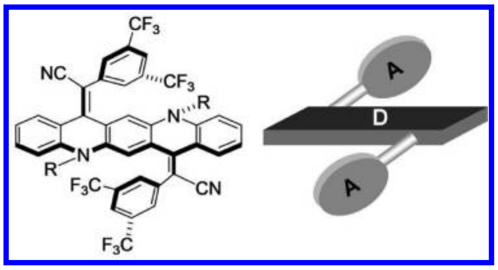

Figure 1. Acceptor−donor−acceptor type quinacridine derivatives.

■ EXPERIMENTAL SECTION

Instrumentation. NMR spectra were recorded on Bruker AVANCE 500 MHz spectrometer with tetramethylsilane as the internal standard. Element analyses and mass spectra were measured on Flash EA 1112 and GC/MS mass spectrometers, respectively. UV−vis absorption spectra were recorded using a PE UV−vis lambdazo spectrometer. To determine the effect of scattering on absorption, the integrated sphere (IS) (an accessory of UV−vis lambdazo spectrometer) was used to measure the absorption spectra. Particles size was determined by dynamic light scattering measurements using Zetasizer Nano-ZS Malvern instruments model ZEN3600. Photoluminescence (PL) spectra were collected on a Shimadzu RF-5301PC spectrophotometer. The microscopy images of as-prepared nano/microwires were obtained on an Olympus BX51 fluorescence microscope. FESEM images were acquired on a JSM 6700F field emission scanning electronic microscope. FETEM images were acquired on a FEI Tecnai G2 F20 S-Twin D573 field emission transmission electronic microscope operated at 200 kV.

Sample Preparation for Photoluminescence Measurements. Small quartz cell with dimensions 0.2 × 1.0 × 4.5 cm^3 was used to accommodate the solution sample. Stock solutions (10^{-4} M) of compounds in THF were primarily prepared. An aliquot of the stock solution was then transferred to a 10 mL volumetric flask, into which an appropriate volume of THF and water was added dropwise under vigorous stirring to furnish 10^{-5} M solutions with different water contents (0−75 vol %). The PL spectra were immediately recorded once the solutions were prepared. The low-temperature PL measurements were performed by using a 5 mm diameter quartz tube that was placed in quartz-walled Dewar flask filled with liquid nitrogen (77 K). The PL quantum yields (Φ_F) of solutions were measured and calculated by employing rhodamine B as standard (Φ_F = 0.50 in ethanol) according to the literature.[19] The solid-state PL quantum yields (Φ_F) measured on Maya2000 Pro CCD spectrometer with an integrating sphere.

X-ray Crystallography. Single crystal suited for X-ray structural analysis was obtained by slow diffusion of petroleum ether into the chloroform solution of **2**. Diffraction data were collected on a Rigaku R-AXIS RAPID diffractometer (Mo Kα radiation, graphite monochromator) in the Ψ rotation scan mode. The structure determination was done with direct methods by using SHELXTL 5.01v and refinements with full-matrix least-squares on F2. The positions of hydrogen atoms were calculated and refined isotropically.

Preparation of Nano- and Microstructures. Organic nanostructures were prepared by using so-called reprecipitation method. The compounds were dissolved in a good solvent THF, resulting in a solution with concentration of 2 × 10^{-3} M. Then 200 μL of the solution was injected into 1 mL of vigorously stirred bad solvent water at 35 °C. One drop of suspension was put onto a silicon wafer and copper grid on different time intervals for SEM and TEM examination. The 1-D micromaterials were prepared by injecting 500 μL of alcohol or chloroform into a 500 μL solution of compounds in THF and casting a drop of solution sample immediately after mixing on glass or silicon substrate followed by slow evaporation typically over 10 h at ambient temperature. FESEM and fluorescence microscopic images were recorded at ambient temperatures.

Materials. Quinacridone was purchased from Tokyo Kasei Kogyo Co. 3,5-Dimethylaniline, 1-bromobutane, 1-bromohexane, and 1-bromooctane were obtained from Acros Organics. Diethyl-2,5-dihydroxy-1,4-dicarboxylate was purchased from Aldrich. The chemicals were used directly without further purification. The C*n*QA (*n* = 4, 6, 8) were synthesized according to the similar method reported in the literature.[20]

Synthesis of 1. To a flask containing 2-(3,5-bis(trifluoromethyl)-phenyl)acetonitrile (0.70 mL, 4 mmol) and triethylamine (TEA) (1.2 mL, 8.5 mmol) dissolved in toluene (20 mL), titanium chloride ($TiCl_4$) (0.6 mL, 5.4 mmol) dissolved in 5 mL of toluene was added dropwise over 15 min by addition funnel under a nitrogen atmosphere. The addition funnel was rinsed with 3 mL of toluene, and then *N,N*′-di(*n*-butyl)quinacridone (C4QA) (0.424 g, 1 mmol) was added by a powder addition funnel. The funnel was rinsed with 3 mL of toluene. The reaction mixture was heated to reflux for 8 h. After cooling to room temperature, the reaction mixture was filtered and the filtrate obtained was dried and purified by column chromatography using silica gel with dichloromethane:diethyl ether (50:1 v:v) as eluent to give 0.491 g of **1** (yield: 55%). ^{1}H NMR ($CDCl_3$, ppm) (500 MHz): δ 8.47 (s, 1 H), 7.70−7.76 (m, 3 H), 7.46 (t, 1 H), 7.35 (d, 1 H), 6.88 (d, 1 H), 6.66−6.75 (m, 1 H), 4.42 (t, 1 H), 3.27−3.37 (m, 1 H), 2.08 (t, 1 H), 1.70−1.75 (m, 1 H), 1.62 (t, 1 H), 1.18 (t, 3 H), 0.84−0.95 (m, 1 H). MS: *m*/*z* 894.26 $[M]^+$. Anal. Calcd for $C_{48}H_{34}$ $F_{12}N_4$ (894.26): C, 64.43; H, 3.83; N, 6.26. Found: C, 64.57; H, 3.98; N, 6.21. Mp 215 °C.

Synthesis of 2. 2-(3,5-Bis(trifluoromethyl)phenyl)acetonitrile (0.70 mL, 4 mmol) reacted with *N,N*′-di(*n*-hexyl)quinacridone (C6QA) (0.480 g, 1 mmol) according to the procedure described for the synthesis of **1** to yield 0.285 g (30%) of **2**. ^{1}H NMR ($CDCl_3$, ppm) (500 MHz): δ 8.46 (s, 1 H), 7.68−7.77 (m, 3 H), 7.45 (t, 1 H), 7.34 (t, 1 H), 6.86 (d, 1 H), 6.64−6.75 (m, 1 H), 4.42 (t, 1 H), 3.26−3.35 (m, 1 H), 1.99−2.10 (m, 1 H), 1.45−1.68 (m, 4 H), 1.25 (t, 2 H), 1.00 (t, 2 H), 0.83−0.95 (m, 2 H), MS: *m*/*z* 950.30 $[M]^+$. Anal. Calcd for $C_{52}H_{42}F_{12}N_4$ (950.30): C, 65.68; H, 4.45; N, 5.89. Found: C, 66.09; H, 4.60; N, 5.93. Mp 184 °C.

Synthesis of 3. 2-(3,5-Bis(trifluoromethyl)phenyl)acetonitrile (0.70 mL, 4 mmol) reacted with *N,N′*-di(*n*-octyle)quinacridone (C6QA) (0.536 g, 1 mmol) according to the procedure described for the synthesis of **1** to yield 0.553 g (55%) of **3**. ^{1}H NMR ($CDCl_3$, ppm) (500 MHz): δ 8.45 (s, 1 H), 7.68−7.75 (m, 3 H), 7.44 (t, 1 H), 7.32 (t, 1 H), 6.88 (d, 1 H), 6.63−6.72 (m, 1 H), 4.42 (t, 1 H), 3.24−3.37 (m, 1 H), 2.00−2.04 (m, 1 H), 1.65 (t, 2 H), 1.60 (t, 2 H), 1.13−1.54 (m, 6 H), 0.91 (t, 3 H), MS: *m*/*z* 1006.30 [M]$^+$. Anal. Calcd for $C_{56}H_{50}F_{12}N_4$: C, 66.79; H, 5.00; N, 5.56. Found: C, 67.01; H, 4.85; N, 5.49. Mp 172 °C.

■ RESULTS AND DISCUSSION

Synthesis. Scheme 1 outlines the synthetic route of the quinacridine-cored A−D−A type compounds **1**−**3**. The precursor alkyl-substituted quinacridones were synthesized according to a standard procedure.[20] The soluble alkyl-substituted quinacridones were treated with 2-(3,5-bis-(trifluoromethyl)phenyl)acetonitrile to form a new series of quinacridine derivatives which were purified by short column with moderate isolate yields (33−55%). These compounds are soluble in common organic solvents, such as toluene, chloroform, and tetrahydrofuran (THF), etc. The chemical structures of **1**−**3** were verified by ^{1}H NMR, mass spectrometry, and element analysis.

Absorption Properties. The absorption spectra of all the compounds were measured both as thin films on quartz and in $CHCl_3$ solution. As shown in Figure 2, these compounds have identical absorption spectrum profile in solution with the same maximum absorption wavelength (λ_{abs} = 572 nm), suggesting that the alkyl chain length does not affect the electronic structure of the conjugated backbones. The λ_{abs} for **1** (571 nm), **2** (575 nm), and **3** (576 nm) in solid thin film are slightly different from each other, suggesting that the alkyl chain may affect the molecular aggregation state, which in turn slightly affects absorption property of thin films. Notably, the spectral profile in the solid state is quite similar to that of solution and the numbers of absorption bands are the same. Hence, one to one correspondence of the absorption bands between the solution and solid state spectra is possible, indicating that the molecular nature is well preserved even in the solid state.

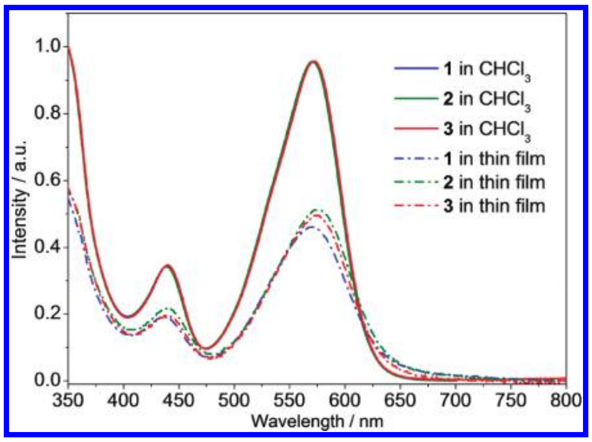

Figure 2. Absorption spectra of compounds **1**−**3** in solutions and thin films.

Aggregation-Induced Emission. The photoluminescence (PL) spectra of **1**−**3** in solution and aggregated states are shown in Figure 3. The emission from the THF solution is so weak that almost no PL signals were recorded when excited at 500 nm. However, dramatic enhancement in luminescence was observed when water as a nonsolvent is added into the THF solution. Since the compounds were insoluble in water, increasing the water fraction in the mixed solvent could change their existing forms (the relative distance between the molecules and geometry of compounds in the solution state) from a solution or well-dispersed state in THF to the aggregated particles in the aqueous THF. The enhanced fluorescence intensity has been attributed to aggregation; therefore, the compounds **1**−**3** were characterized as AIE active. Changes in the PL peak intensity versus water fraction of the mixture for all compounds are plotted as an inset in Figure 3. As the water fraction was increased from 0 to 75%, the fluorescence intensity has increased many folds. It is worthy to note that this enhancement was not the same for all compounds. To have a quantitative picture, we have estimated the fluorescence quantum yields (Φ_F) of the THF solutions, THF/water mixtures, and solid thin films of the compounds

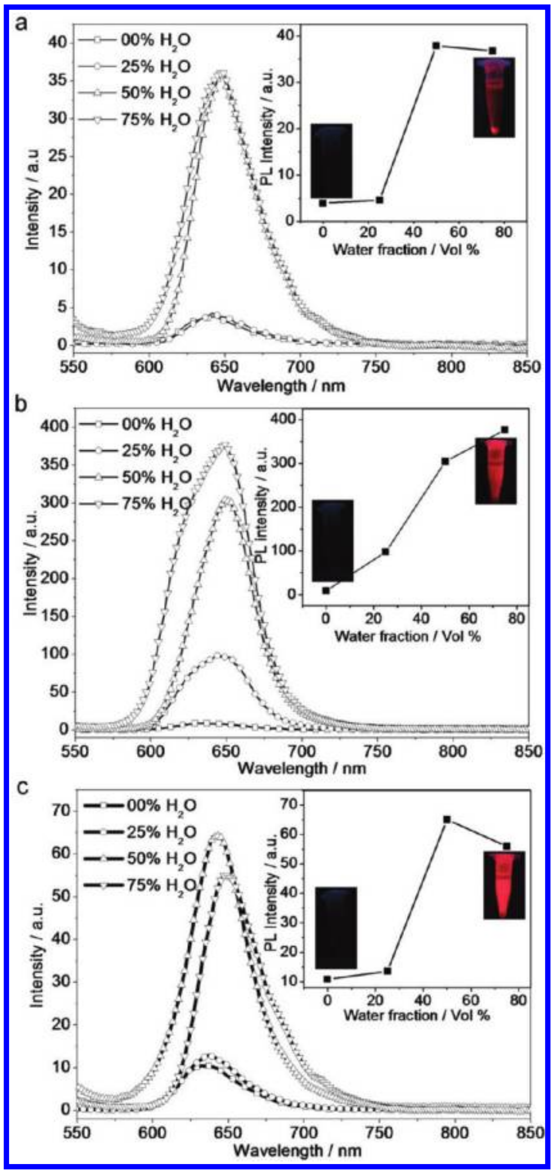

Figure 3. PL spectra of **1** (a), **2** (b), and **3** (c) with different water fractions and fluorescence emission image (0 and 50% H_2O) under 500 nm excitation.

using rhodamine B as a standard. The fluorescence quantum yield (Φ_F) for **1**, **2**, and **3** in THF are 2.1×10^{-4}, 2.3×10^{-4}, and 2.6×10^{-4}, respectively, which has significantly increased to 8.9×10^{-3}, 9×10^{-2}, and 9.5×10^{-2} in a THF/H_2O (1:1 v:v) mixture and 1.0×10^{-2}, 9.9×10^{-2}, and 1.0×10^{-1} in solid films.

Effect of Polar Structural Units on AIE. The molecules without polar structural units excluded the involvement of J- and H-aggregates effect in their PL proceses.[21,22] Such AIE molecules emits in the short wavelength region and emits blue light in the aggregated state due to the absence D−A interactions in the systems.[23,24] Although alkyl-substituted QA derivatives are not AIE active, their electron-donating feature and twisted structure after substituting with 2-(3,5-bis(trifluoromethyl)phenyl)acetonitrile units make QA molecules are useful central core for constructing organic molecules with AIE property. Compounds **1**−**3** with QA skeleton as a donor unit and 2-(3,5-bis(trifluoromethyl)phenyl)acetonitrile as acceptor units make them AIE active. Generally, the emission wavelength and color of AIE molecules without polar units are scarcely affected by solvent polarity. Molecules with intramolecular charge transfer nature like compounds **1**−**3** can bathochromically shifted their fluorescence with increasing solvent polarity due to that polar solvents alter their ground and excited states and narrow their energy gaps.[25,26]

Concentration Dependence of the Aggregation-Induced Emission. The concentration-dependent emission property of compound **2** in THF/H_2O (1:1 v:v) mixture has been studied (Figure S1). Upon concentration increasing, the emission intensity decreased significantly and the emission maximum displayed a red-shift. Compound **2** was unsolvable in H_2O, the increase of concentration of **2** could reduce the solvating power, which resulted in enhancement of aggregation and increase of the particle size. As the particle size increase, the emission intensity should decrease and the emission maximum shift to longer wavelength.[27] To support above explanation, the particle size measurement has been performed. The dynamic light scattering (DLS) experimental results showed that the average diameters of particles for different concentrations were 340 nm (1×10^{-4} M), 375 nm (1.5×10^{-4} M), 415 nm (2×10^{-4} M), 463 nm (2.5×10^{-4} M), and 601 nm (3×10^{-4} M). For the solution systems with large size organic particles, their emission and absorption properties may be influenced by the scattering of the organic particles.[28] The emission spectra presented in Figure S1 have been obtained based on the excitation wavelength of 500 nm. Therefore, the scattering of excitation light has no effect on the emission spectra that appears beyond 600 nm. The concentration-dependent absorption spectra that have been recorded by integrated sphere and normal transmission method are presented in Figure S2. There is no significant effect of scattering on the absorbance, except for the 3×10^{-4} M THF/H_2O mixture. For the absorption spectra measured by integrated sphere, the effect of scattering can be eliminated.

Effect of Temperature on Molecular Rotations. It is known that that rotational energy relaxation can nonradiatively deactivate the excited specie and result in weakening the corresponding fluorescence.[29] In the dilute solutions, the active molecular rotations may effectively decimate the excited exciton through molecular collision with solvent molecules, thus making the fluorescent molecules nonemissive. In the solid aggregates, the stacking forces among the aromatic fluorophores may restrict the molecular rotations which block the nonradiative channels and populate the radiative decay. As molecular rotations can be thermally activated, the effect of molecular rotations on emission behavior can be appraised by examining the temperature-dependent emission spectra.

The temperature-dependent PL spectra of dilute solutions of compounds **1**−**3** in THF were measured (Figure 4). It is noted that at room temperature all compounds have very faint emission or almost no emission. At −196 °C, these compounds show intense emission peak due to the blockage of molecular rotations. As the temperature is increased, the emission intensity tend to decrease, but there is a dramatic abrupt decrease in the emission intensity at the melting point of the solvent (−108 °C) due to free molecular rotations which deactivate the excited specie through the nonradiative way. The extent of decrease at the melting temperature was not the same for all compounds. The PL intensities of **1**, **2**, and **3** at −196 °C

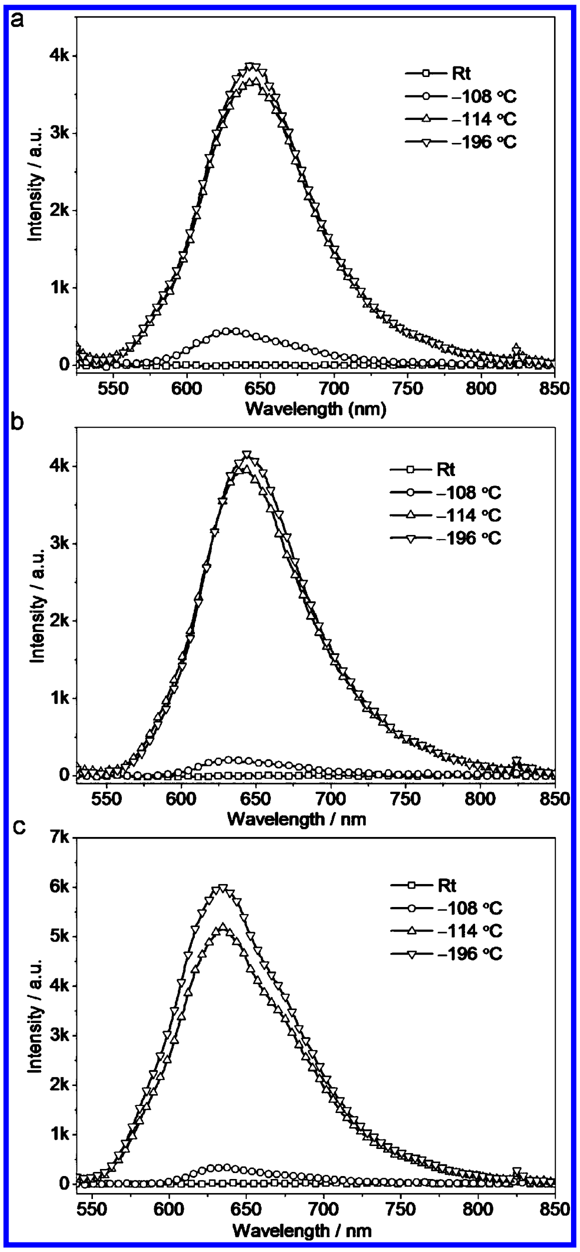

Figure 4. Emission of **1** (a), **2** (b), and **3** (c) in THF at variable temperature.

are 9-, 18-, and 19-fold higher than those at −108 °C. The extent of decrease seems to be closely related to the steric effect of QA skeleton. As compounds **2** and **3** have a longer alkyl chain length than **1**, so they have more steric effect making the rotation difficult at low temperatures.

Morphology Transition from 0-D Nanostructures to 1-D Microwires. It is demonstrated that molecular structures containing π-conjugated rigid core and soft alkyl chains could be suitable to prepare 1-D nanostructures for the application of photoelectric nanodevices.[30] The molecular structure shown in Figure 1 reveals that all molecules with π-conjugated rigid cores and two alkyl chains may have one-dimensional self-assembly property. Figure 5 shows the morphological transition of the compound **2** in THF/H_2O mixture solution. The nanoparticles with opening holes on their surfaces have been observed when the sample was collected on the silicon wafers immediately after injecting 200 μL of THF solution (1×10^{-3} M) into 1 mL of well-stirred water (Figure 5a,b). The diameters of the hollow spheres range from 300 to 530 nm. It was revealed that the vesicles were not separately dispersed, and their edges were cohered. The membranes of these vesicles were shared, and those between fused vesicles were eroded. This behavior suggested a growing tendency of the vesicles. To further investigate this trend, we prepared the samples after aging in the combined THF/H_2O solvent system for 10 min and collected the intermediate states of the morphology transition. SEM images of the intermediates showed that the vesicles were arranged one-by-one in a linear way (Figure 5c,d). Some of the membranes between the vesicles started forming a tubular structure (Figure 5e). The SEM images of the sample prepared after 30 min of aging in the combined solvent showed large-scale 1-D nanostructures, which indicates the 1-D growing tendency of the vesicles (Figure 5f,g). When the samples were kept at ambient conditions for 1 day, the globular nanotubes have transformed into long microwires with diameter of 350 nm (Figure 5h). The only difference between samples with the two different morphologies is that they underwent different aging time, so we can infer that the 1-D nanostructures were grown from the initially formed vesicles. To clarify the structure of the vesicles and nanotubes, the transmission electron microscope (TEM) measurements (Figure S3) have been performed and provided enough evidence for above discussions.

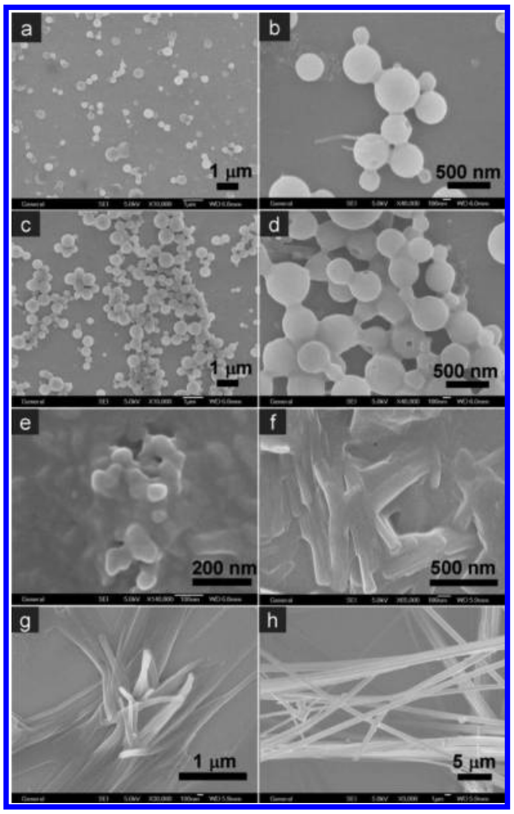

Figure 5. (a−c) SEM images of large-scale vesicles collected immediately after injecting solution in THF into well-stirred H_2O. (d−g) SEM images of intermediates of morphology transition. (h) SEM final image of 1D microwire.

At this stage the mechanism of the formation of vesicles remains poorly understand. A possible explanation for this phenomenon is that for the compounds **1−3** segregation by high solvophobic nature of the trifluoromethyl groups may actuate the molecules assemble into layered structures and finally close to form vesicles.[31] The tube formation progress in this study may be similar to the "curvature strain releasing" process proposed by Rowan and Nolte which explain the fusion of PS-PIAT from small vesicles to larger ones.[32] There is large number of membrane defects and high curvature in the initially formed vesicles. These membrane defects results in the fusion of vesicles during which curvature energy is released which results in thermodynamically more stable tubular structure. As THF erode the membrane, therefore, it plays an essential role in the tubular formation. This might be proved by the fact that no morphology transition would happen if the vesicles were collected from the suspension and the solvents were allowed to evaporate.

1D Self-Assembly. Beside the above-mentioned reprecipitation process, the solution evaporation approach was also employed to fabricate compounds **1−3** molecules into luminescent wires. The experimental results demonstrated that solution evaporation process leaded to the formation of luminescent wires with larger diameters than reprecipitation approach. Size controllable well-defined 1-D microwires have been obtained by injecting 500 μL of alcohol into a 500 μL THF solution (1×10^{-3} M) and casting a drop of sample on silicon substrate followed by slow evaporation typically over 10 h at ambient temperature. Fluorescence microscopic images and SEM images revealed that 1-D microwires with different length and diameter have been generated for all compounds. It is worth mentioning that the short alkyl chain alcohol with fast evaporation process leads to a random morphology with irregular size and shape. Interestingly, relatively uniform ultralong microwires with high aspect ratio were obtained when *n*-butanol or *n*-pentanol was injected into THF solution due to slow evaporation of the solvents. The experimental results demonstrated that the evaporation of the THF/*n*-butanol solution of compound **1** led to the formation of luminescent wires with small aspect ratio (diameter of 2 μm and length up to about 200 μm) (Figure 6). Compounds **2** and **3** with longer alkyl chain could assemble into more uniform and elongated microwires. Compound **2** generated rodlike microwires with a diameter of 4 μm and length of more than 500 μm (Figure 7). It is worth noting that microwires generated by the slow evaporation of THF/*n*-pentanol and $CHCl_3$/*n*-butanol solutions of compound **2** were more elongated rodlike wires with length of more than 1000 μm and diameter of 4 μm. Interestingly, compound **3** has formed highly luminescent

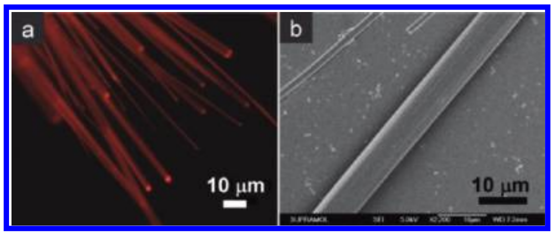

Figure 6. Fluorescence microscopic images (a) and FESEM images (b) of microwires of compound **1** prepared by the slow evaporation process.

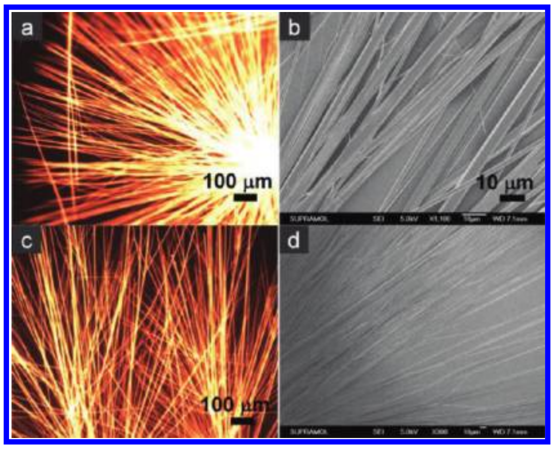

Figure 7. Fluorescence microscopic images (a) of microwires of compound **2** prepared from the THF/*n*-butanol solution and (c) $CHCl_3$/*n*-butanol solution. FESEM images (b) of microwires of compound **2** prepared from the THF/*n*-butanol solution and (d) $CHCl_3$/*n*-butanol solution by the slow evaporation process.

ultralong and thin 1-D microwires with a diameter of 700 nm and length of several millimeters (Figure 8).

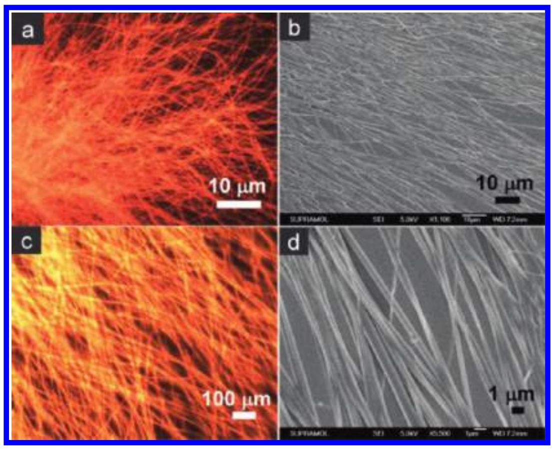

Figure 8. Fluorescence microscopic images (a) of microwires of compound **3** prepared from the THF/*n*-butanol solution and (c) prepared from THF/*n*-pentanol by the slow evaporation process; FESEM images (b) of microwires prepared from THF/*n*-butanol and (d) prepared from the THF/*n*-pentanol by the slow evaporation process.

Effect of Morphology on Luminescent Properties. Comparing the emission behavior (Figure S4) of nano/microwires generated from chloroform/*n*-butanol solution of **2** by the slow evaporation process (for instance), powder sample (a mixture of crystals and amorphous solid) formed from chloroform/pentane, and nanoaggregates in THF/H_2O (1:1 v:v) mixture, it was found that the nano/microwires displayed the shortest emission maximum and nanoaggregates showed the longest one. The emission maximum of powder sample located between those of nano/microwires and nanoaggregates. The powder sample exhibited obviously weaker emission compared with nano/microwires and nanoaggregates. The nanoaggregates generated in THF/H_2O mixture often have normally both amorphous and crystalline phases,[33] which may allow the molecules adopt multiconfigurations. On the other hand, in the nano/microwires all of the molecules adopt the same configuration or very similar configuration. Therefore, microwires showed the shortest emission maximum. The molecular configuration and packing feature of the powder sample may lie between nano/microwires and nanoaggregates. Shoulder peaks are observed for the powders and nano/microwires. The shape of the spectrum of the nanoaggregates is somewhat skewed, which can be attributed to strong light absorption by the red tail of the absorption band.

Crystal Structure. To further explore AIE and 1-D self-assembly properties of the present A–D–A type compounds, molecular conformation as well as intermolecular interactions in the solid state are really important. All the compounds were subjected to single crystal growth; however, only compound **2** produced crystals that could be subjected to X-ray diffraction. As depicted in Figure 9a, the crystal structure demonstrates that the central quinacridine core is heavily bent from the planar conformation and the whole molecule has a highly twisted structure. This twisted structure is stabilized by multiple intermolecular hydrogen-bonding interactions (totally 11 hydrogen bonds for each molecule) including $C{-}H(CH_2){\cdots}N$-(core), $C{-}H(Ph){\cdots}N(CN)$, $C{-}H(CH_2){\cdots}F$, and $C{-}H$-$(Ph){\cdots}F$. The hydrogen bond interaction involving 2-(3,5-bis(trifluoromethyl)phenyl)acetonitrile interlocks the free rotations of 2-(3,5-bis(trifluoromethyl)phenyl)acetonitrile along the bond between olefinic carbon and phenyl carbon,

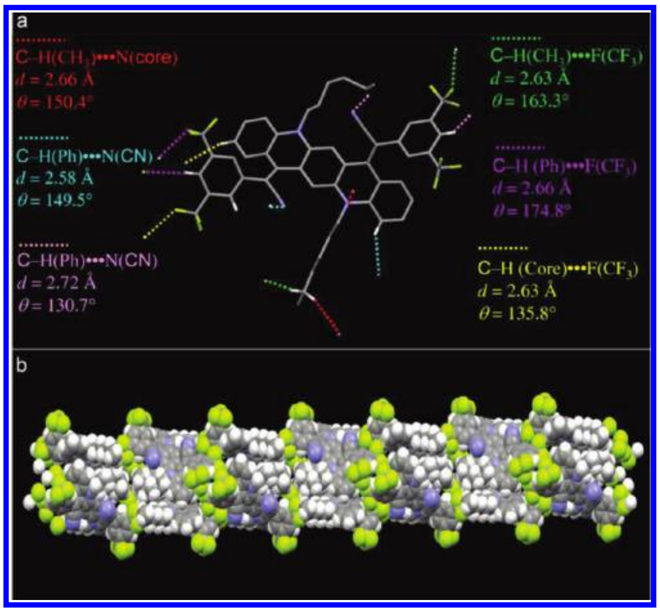

Figure 9. Molecular structure and intermolecular hydrogen-bonding interactions (a) and 1-D molecular packing structure constructed by the hydrogen bonds of outer trifluoromethylphenyl groups (b).

which reduces the nonradiative decay pathways through interactions among the neighboring molecules. It is also important to note that core skeleton adopts nonplanar geometry and rather buckled shape which inhibits face-to-face molecular stacking, too. Therefore, the abundant intermolecular interactions can enhance the rigidity of these compounds and may be an advantage to the emission of aggregation state.

The intermolecular interactions of the outer 3,5-bis(trifluoromethyl)phenyl groups, which may determine the self-assembly feature of the bulk sample, make molecules stack into 1-D molecular columns, as shown in Figure 9b. Such a packing structure implies that these types of molecules have a natural tendency to aggregate into linear 1-D structures. The single-crystal structure of compound **2** therefore provides a rational explanation for the formation of 1-D microfibers. To evaluate the molecular structure and packing structure of the self-assembly structures, X-ray diffraction (XRD) patterns of microwires constructed by compound **2** and that of single crystal of compound **2** calculated from single crystal data were compared (Figure S5). The XRD patterns of the microwires are similar to the XRD pattern of single crystal which suggests that molecular packing of the fibers is analogous to that in a single crystal of **2**.

■ CONCLUSIONS

Quinacridine derivatives **1−3** synthesized by introducing 2-(3,5-bis(trifluoromethyl)phenyl)acetonitrile at the carbonyl position of alkyl-substituted quinacridones exhibited aggregation-induced-emission (AIE) and 1D self-assembly properties. It was found that 2-(3,5-bis(trifluoromethyl)phenyl)acetonitrile units in these derivatives play a vital role in 1-D self-assembly of the molecules. All these as-synthesized AIE-active compounds are red emitting in the aggregated state. These compounds are also luminescent at low solution temperature, indicating that restricted intramolecular rotation is the key factor in deciding AIE effect. These compounds have been employed to fabricate organic 1-D luminescent nano- and microwires based on reprecipitation or slow evaporation approaches. The morphological transition from zero-dimensional (0-D) hollow nanospheres to one-dimensional (1-D) nano- and micromaterials was observed by taking SEM and TEM images of the samples collected in THF/H_2O mixtures at different aging times. The single-crystal structure of one compound provides a rational explanation for the 1-D self-assembly feature of the present compounds.

■ ASSOCIATED CONTENT

Ⓢ Supporting Information

XRD pattern of compound **2**, emission spectra of compound **2** at different concentration in THF/H_2O mixture, emission spectra of amorphous powder, nano/microwires and nanoaggregates of compound **2**, TEM images of morphology transition, and crystallographic data. This material is available free of charge via the Internet at http://pubs.acs.org.

■ AUTHOR INFORMATION

Corresponding Author

*Fax: +86-431-85193421. E-mail: hongyuzhang@jlu.edu.cn (H.Z.); yuewang@jlu.edu.cn. (Y.W.).

■ ACKNOWLEDGMENTS

This work was supported by the National Natural Science Foundation of China (50773027 and 50733002), the Major State Basic Research Development Program (2009CB939700), and 111 Project (B06009).

■ REFERENCES

(1) (a) Shah, P. S.; Hanrath, T.; Johnston, K. P.; Korian, B. A. *J. Phys. Chem. B* **2004**, *108*, 9574. (b) Hayden, O.; Payne, C. K. *Angew. Chem., Int. Ed.* **2005**, *44*, 1395. (c) Duan, X.; Huang, Y.; Cui, Y.; Wang, J.; Lieber, C. M. *Nature* **2001**, *409*, 66.

(2) (a) Henglein, A. *Chem. Rev.* **1989**, *89*, 1861. (b) Burda, C.; Chen, X. B.; Narayanan, R.; El-Sayed, M. A. *Chem. Rev.* **2005**, *105*, 1025. (c) Moriarty, P. *Rep. Prog. Phys.* **2001**, *64*, 297. (d) Peng, X. G.; Schlamp, M. C.; Kadavanich, A. V.; Alivisatos, A. P. *J. Am. Chem. Soc.* **1997**, *119*, 7019. (e) Chan, W. C. W.; Nie, S. M. *Science* **1998**, *281*, 2016.

(3) (a) Xia, Y. N.; Yang, P. D.; Sun, Y. G.; Wu, Y. Y.; Mayers, B.; Gates, B.; Yin, Y. D.; Kim, F.; Yan, H. Q. *Adv. Mater.* **2003**, *15*, 353. (b) Hu, J. T.; Odom, T. W.; Lieber, C. M. *Acc. Chem. Res.* **1999**, *32*, 435.

(4) (a) Naddo, T.; Che, Y.; Zhang, W.; Balakrishnan, K.; Yang, X.; Yen, M.; Zhao, J.; Moore, J. S.; Zang, L. *J. Am. Chem. Soc.* **2007**, *129*, 6978. (b) Che, Y.; Datar, A.; Balakrishnan, K.; Zang, L. *J. Am. Chem. Soc.* **2007**, *129*, 7234. (c) Che, Y.; Yang, X.; Loser, S.; Zang, L. *Nano Lett.* **2008**, *8*, 2219. (d) Che, Y.; Yang, X.; Zang, L. *Chem. Commun.* **2008**, 1413. (e) Che, Y. K.; Zang, L. *Chem. Commun.* **2009**, 5106.

(5) (a) Dautel, O. J.; Wantz, G.; Almairac, R.; Flot, D.; Hirsch, L.; Lere-Porte, J.-P.; Parneix, J.-P.; Serein-Spirau, F.; Vignau, L.; Moreau, J. J. E. *J. Am. Chem. Soc.* **2006**, *128*, 4892. (b) Zhao, Y. S.; Di, C.; Yang, W.; Yu, G.; Liu, Y.; Yao, J. *Adv. Funct. Mater.* **2006**, *16*, 1985. (c) Zhao, Y. S.; Fu, H.; Hu, F.; Peng, A.; Yang, W.; Yao, J. *Adv. Mater.* **2008**, *20*, 79. (d) Datar, A.; Balakrishnan, K.; Yang, X.; Zuo, X.; Huang, J.; Oitker, R.; Yen, M.; Zhao, J.; Tiede, D. M.; Zang, L. *J. Phys. Chem. B* **2006**, *110*, 12327. (d) Lei, Y. L.; Liao, Q.; Fu, H. B.; Yao, J. N. *J. Am. Chem. Soc.* **2010**, *132*, 1742. (e) Wang, X.; Yan, J.; Zhou, Y.; Pei, J. *J. Am. Chem. Soc.* **2010**, *132*, 15872. (f) Kang, L. T.; Fu, H. B.; Cao, X. Q.; Shi, Q.; Yao, J. N. *J. Am. Chem. Soc.* **2011**, *133*, 1895. (g) Liao, Q.; Fu, H. B.; Wang, C.; Yao, J. N. *Angew. Chem., Int. Ed.* **2011**, *50*, 4942. (h) Zhang, C.; Zheng, J.; Zhao, Y. S.; Yao, J. N. *Adv. Mater.* **2011**, *23*, 1380.

(6) (a) Bao, Z.; Lovinger, A. J.; Dodabalapur, A. *Appl. Phys. Lett.* **1996**, 3066. (b) Briseno, A. L.; Mannsfeld, S. C. B.; Reese, C.; Hancock, J. M.; Xiong, Y.; Jenekhe, S. A.; Bao, Z.; Xia, Y. *Nano Lett.* **2007**, *7*, 2847. (c) Che, Y.; Datar, A.; Yang, X.; Naddo, T.; Zhao, J.; Zang, L. *J. Am. Chem. Soc.* **2007**, *129*, 6354.

(7) (a) Takazawa, K.; Kitahama, Y.; Kimura, Y.; Kido, G. *Nano Lett.* **2005**, *5*, 1293. (b) Yanagi, H.; Morikawa, T. *Appl. Phys. Lett.* **1999**, *75*, 187. (c) Balzer, F.; Bordo, V. G.; Simonsen, A. C.; Rubahn, H. G. *Appl. Phys. Lett.* **2003**, *82*, 10. (d) Quochia, F.; Cordella, F.; Mura, A.; Bongiovanni, G.; Balzer, F.; Rubahn, H. G. *Appl. Phys. Lett.* **2006**, *88*, 041106. (e) Zhao, Y. S.; Xu, J.; Peng, A.; Fu, H.; Ma, Y.; Jiang, L.; Yao, J. *Angew. Chem., Int. Ed.* **2008**, *47*, 7301. (f) Zhao, Y. S.; Peng, A.; Fu, H.; Ma, Y.; Yao, J. *Adv. Mater.* **2008**, *20*, 1661. (g) Giansante, C.; Raffy, G.; Schafer, C.; Rahma, H.; Kao, M. T.; Olive, A. G. L.; Guerzo, A. D. *J. Am. Chem. Soc.* **2011**, *133*, 316. (h) Zhang, X. J.; Zhang, X. H.; Zou, K.; Lee, C. S.; Lee, S. T. *J. Am. Chem. Soc.* **2007**, *129*, 3527.

(8) (a) Yamamoto, Y.; Fukushima, T.; Sun, Y.; Ishii, N.; Saeki, A.; Seki, S.; Tagawa, S.; Taniguchi, M.; Kawai, T.; Aida, T. *Science* **2006**, 1761. (b) Schwab, A. D.; Smith, D. E.; Bond-Watts, B.; Johnston, D. E.; Hone, J.; Johnson, A. T.; de Paula, J. C.; Smith, W. F. *Nano Lett.* **2004**, 1261. (c) Zhang, X.; Jie, J.; Zhang, W.; Zhang, C.; Luo, L.; He, Z.; Zhang, X.; Zhang, W.; Lee, C.; Lee, S. *Adv. Mater.* **2008**, *20*, 2427. (d) Ji, H. X.; Hu, J.-S.; Wan, L. J. *Chem. Commun.* **2008**, 2653.

(9) (a) Schmidt-Mende, L.; Fechtenkötter, A.; Müllen, K.; Moons, E.; Friend, R. H.; MacKenzie, J. D. *Science* **2001**, *293*, 1119. (b) Hasobe, T.; Imahori, H.; Fukuzumi, S.; Kamat, P. V. *J. Mater. Chem.* **2003**, *13*, 2515.

(10) (a) Würthner, F. *Chem. Commun.* **2004**, 1564. (b) Hoeben, F. J. M.; Jonkheijm, P.; Meijer, E. W.; Schenning, A. P. H. J. *Chem. Rev.* **2005**, *105*, 1491. (c) Grimsdale, A. C.; Müllen, K. *Angew. Chem., Int. Ed.* **2005**, *44*, 5592. (d) *Supramolecular Dye Chemistry*; Würthner, F., Ed.; Topics in Current Chemistry; Springer: Berlin, 2005; Vol. 258. (e) Zang, L.; Che, Y.; Moore, J. S. *Acc. Chem. Res.* **2008**, *41*, 1596−1608. (f) Zhao, Y. S.; Fu, H.; Peng, A.; Ma, Y.; Xiao, D.; Yao, J. *Adv. Mater.* **2008**, *20*, 2859.

(11) (a) Balakrishnan, K.; Datar, A.; Naddo, T.; Huang, J.; Oitker, R.; Yen, M.; Zhao, J.; Zang, L. *J. Am. Chem. Soc.* **2006**, *128*, 7390. (b) Johnson, C. A.; Sharma, S.; Subramaniam, B.; Borovik, A. S. *J. Am. Chem. Soc.* **2005**, *127*, 9698. (c) Wang, Y.; Fu, H.; Peng, A.; Zhao, Y.; Ma, J.; Ma, Y.; Yao, J. *Chem. Commun.* **2007**, 1623. (d) Su, W.; Zhang, Y.; Zhao, C.; Li, X.; Jiang, J. *ChemPhysChem* **2007**, *8*, 1857.

(12) Girouard, S.; Houle, M. H.; Grandbois, A.; Keillor, J. W.; Michnick, S. W. *J. Am. Chem. Soc.* **2005**, *127*, 559.

(13) Parak, W. J.; Pellegrino, T.; Plank, C. *Nanotechnology* **2005**, *16*, R9.

(14) (a) Luo, J.; Xie, Z.; Lam, J. W. Y.; Cheng, L.; Tang, B. Z.; Chen, H.; Qiu, C.; Kwok, H. S.; Zhan, X.; Liu, Y.; Zhu, D. *Chem. Commun.* **2001**, 1740. (b) Ren, Y.; Lam, J. W. Y.; Dong, Y.; Tang, B. Z.; Wong, K. S. *J. Phys. Chem. B* **2005**, *109*, 1135−1140. (c) Yuan, W. Z.; Lu, P.; Chen, S. M.; Lam, J. W. Y.; Wang, Z. M.; Liu, Y.; Kwok, H. S.; Ma, Y. G.; Tang, B. Z. *Adv. Mater.* **2010**, *22*, 2159.

(15) (a) Wang, Z.; Shao, H.; Ye, J.; Tang, L.; Lu, P. *J. Phys. Chem. B* **2005**, *109*, 19627. (b) Liu, Y.; Tao, X.; Wang, F.; Shi, J.; Sun, J.; Yu, W.; Ren, Y.; Zou, D.; Jiang, M. *J. Phys. Chem. C* **2007**, *111*, 6544.

(16) Tong, H.; Dong, Y.; Häussler, M.; Hong, Y.; Lam, J. W. Y.; Sung, H. H-Y.; Williams, I. D.; Kwok, H. S.; Tang, B. Z. *Chem. Phys. Lett.* **2006**, *428*, 326.

(17) (a) Xu, J.; Liu, X.; Lv, J.; Zhu, M.; Huang, C.; Zhou, W.; Yin, X.; Liu, H.; Li, Y.; Ye, J. *Langmuir* **2008**, *24*, 4231. (b) An, B. K.; Gihm, S. H.; Chung, J. W.; Park, C. R.; Kwon, S. K.; Park, S. Y. *J. Am. Chem. Soc.* **2009**, *131*, 3950.

(18) (a) Zhao, Y. F.; Mu, X. Y.; Bao, C. X.; Fan, Y.; Zhang, J. Y.; Wang, Y. *Langmuir* **2009**, *25*, 3264. (b) Wang, J.; Zhao, Y. F.; Zhang, J. H.; Zhang, J. Y.; Yang, B.; Wang, Y.; Zhang, D. K.; You, H.; Ma, D. G. *J. Phys. Chem. C* **2007**, *111*, 9177.

(19) Donegá, C.; de, M.; Hickey, S. G.; Wuister, S. F.; Vanmaekelbergh, D.; Meijerink, A. *J. Phys. Chem. B* **2003**, *107*, 489.

(20) (a) Keller, U.; Müllen, K.; De Feyter, S.; De Schryver, F. C. *Adv. Mater.* **1996**, *8*, 490. (b) De Feyter, S.; Gesquière, A.; De Schryver, F. C.; Keller, U.; Müllen, K. *Chem. Mater.* **2002**, *14*, 989.

(21) Chen, J.; Law, C. C. W.; Lam, J. W. Y.; Dong, Y.; Lo, S. M. F.; Williams, I. D.; Zhu, D.; Tang, B. Z. *Chem. Mater.* **2003**, *15*, 1535.

(22) Yu, G.; Yin, S.; Liu, Y.; Chen, J.; Xu, X.; Sun, X.; Ma, D.; Zhan, X.; Peng, Q.; Shuai, Z.; Tang, B. Z.; Zhu, D.; Fang, W.; Luo, Y. *J. Am. Chem. Soc.* **2005**, *127*, 6335.

(23) Yang, Z.; Chi, Z.; Yu, T.; Zhang, X.; Chen, M.; Xu, B.; Liu, S.; Zhang, Y.; Xu, J. *J. Mater. Chem.* **2009**, *19*, 5541.

(24) Hirano, K.; Minakata, S.; Komatsu, M.; Mizuguchi, J. *J. Phys. Chem. A* **2002**, *106*, 4868.

(25) (a) Rettig, W. *Angew. Chem., Int. Ed. Engl.* **1986**, *25*, 971. (b) Grabowski, Z. R.; Rotkiewicz, K.; Rettig, v. *Chem. Rev.* **2003**, *103*, 3899.

(26) Tong, H.; Dong, Y.; Haeussler, M.; Hong, Y.; Lam, J. W. Y.; Sung, H. H. Y.; Williams, I. D.; Kwok, H. S.; Tang, B. Z. *Chem. Phys. Lett.* **2006**, *428*, 326.

(27) Fu, H. B.; Yao, J. N. *J. Am. Chem. Soc.* **2001**, *123*, 1434.

(28) Ishino, H.; Nair, S. V.; Nakagawa, K.; Kobayashi, T.; Tokunaga, E. *Appl. Phys. Lett.* **2011**, *99*, 053304.

(29) (a) Wong, K. S.; Wang, H.; Lanzant, G. *Chem. Phys. Lett.* **1998**, *288*, 59. (b) Malyukin, Y. V. *J. Phys. Chem. C* **2008**, *112*, 14762.

(30) Hoeben, F. J. M.; Jonkheijm, P.; Meijer, E. W.; Schenning, A. P. H. J. *Chem. Rev.* **2005**, *105*, 1491.

(31) Bhosale, S. V.; Jani, C.; Lalander, C. H.; Langford, S. J. *Chem. Commun.* **2010**, *46*, 973.

(32) Vriezema, D. M.; Hoogboom, J.; Velonia, K.; Takazawa, K.; Christianen, P. C. M.; Maan, J. C.; Rowan, A. E.; Nolte, R. J. M. *Angew. Chem., Int. Ed.* **2003**, *42*, 772.

(33) Dong, Y.; Lam, J. W. Y.; Qin, A.; Li, Z.; Sun, J.; Sung, H. H. Y.; Williams, I. D.; Tang, B. Z. *Chem. Commun.* **2007**, 40.